Article

Correlating the Process Variables and Products Involved in the Fluid Catalytic Cracking of Waste Feeds

José Ignacio Alvira†, Idoia Hita†, Elena Rodríguez, José M. Arandes, Pedro Castaño*

Department of Chemical Engineering, University of the Basque Country UPV/EHU, P.O. Box 644, 48080. Bilbao, Spain.

* Correspondence: pedro.castano@ehu.eus; Tel.: +34-94601-8435

Abstract: Associating the most influential parameters with the product distribution is of uttermost importance in complex catalytic processes such as fluid catalytic cracking (FCC). These correlations can lead to the information-driven catalyst screening, kinetic modeling and reactor design. In this work, a dataset of 104 uncorrelated experiments, with 64 variables, has been obtained in an FCC simulator using 6 types of feedstock (vacuum gasoil, polyethylene pyrolysis waxes, scrap tire pyrolysis oil, dissolved polyethylene and blends of the previous), 36 possible sets of conditions (varying contact time, temperature and catalyst/oil ratio) and 3 industrial catalysts. Principal component analysis (PCA) has been applied over the dataset, showing that the main components are associated with feed composition (27.41% variance); operational conditions (19.09%) and catalyst properties (12.72%). The variables of each component have been correlated with the indexes and yields of the products: conversion, octane number, aromatics, olefins (propylene) or coke, among others.

Keywords: principal component analysis (PCA); fluid catalytic cracking (FCC); waste valorization; scrap tires; polyolefin pyrolysis

1. Introduction

The global requirement for transportation fuels is expected to grow steadily over the coming years due to an increasing demand of energy from developed and developing countries [1]. The foreseeable petroleum depletion will be anticipated by the use of heavier and low-quality crudes, together with a switch of market demand from heavy-fuel fractions towards gasoline and light olefins. These combined aspects justify the current necessity of refineries to evolve by introducing new units, revamping used ones and varying the feedstock in order to expand their versatility and capacity [2].

The fluid catalytic cracking (FCC) unit plays a key role in an integrated and intensified refinery as the primary catalytic conversion process (in terms of volume) greatly determining its competitiveness and margin [3]. In the recent years, important efforts have been directed towards the improvement of these highly demanding units [4]. The underlaying drive of these works highlight the essential role of the FCC unit in the path towards an integrated waste and bio-refinery concept [5–7]. FCC units have traditionally processed heavy petroleum fractions (vacuum gas oil, VGO) into interesting products such as gasoline, diesel or propylene [8,9]. However, taking the remarkable versatility of FCC, other non-conventional feeds have been studied [10]: (i) secondary refinery streams, (ii) streams derived from the consumer society, or (iii) oxygenated bio-derived feedstock. As secondary refinery streams (i), Arandes et al. [11,12] studied the effect of co-feeding atmospheric distillation residue (20 wt%) with VGO in a riser simulator, observing a crucial role of the reactant accessibility for the efficient conversion of bulky aromatic molecules, and also the great influence of the temperature and catalyst/oil (C/O) ratio on gasoline composition. Garcia et al. [13] observed an

improvement of conversion of the blend of atmospheric distillation residue (10 wt%) and VGO, compared with the VGO alone. Specifically, these authors observed a higher yield of light cycle oil (LCO) at the price of slightly faster coke formation with the blend. As streams derived from the consumer society (ii), waste polyolefins have an ideal composition as FCC feedstock and their valorization can be carried out either dissolving the polymer in the feed [14,15], or performing a previous pyrolysis [16–19]. Lovás et al. [20] compared the catalytic cracking in FCC conditions of high-density polyethylene (HDPE) and polypropylene (PP) waxes together with VGO and it was concluded that PP should be used preferentially in order to boost gasoline production. On the other hand, the condensed pyrolysis oil derived from waste (scrap) tires also shows great prospects to become a FCC feed and produce high quality fuels [21–23]. Concerning oxygenated bio-derived streams (iii), a great research interest towards exploring the possibilities of bio-derived feedstock (i.e. bio-oil, vegetable oils) for FCC conversion has been studied [24–30].

Despite the effort, a proper assessment of the effect of set of conditions (feed, catalyst, operational conditions) on the results is challenging due to the great number of correlated and uncorrelated variables affecting the system [31]. In this context, principal component analysis (PCA) is a valuable statistical tool that can aid the process design by replacing a large set of variables with a smaller set of new variables (principal components) that describe the observed patterns [32–34]. To date, PCA has been used in the oil industry as a predictive tool for the determination of process monitoring and control [35], fault discovery [36], reactor modeling [37], determination of physical properties of petroleum samples [38], catalyst characterization [39] and for gathering insight into catalyst behavior and classification of the main reaction routes in the catalytic cracking of decalin over Y-zeolites [40]. The application of this method has also been reported for the evaluation of the optimal reaction conditions for the catalytic oxidation of toluene [41] as well as for proposing kinetic schemes in the thermal pyrolysis of waste HDPE plastics [42] and waste tires [43]. Pasadakis et al. [39] have used the PCA methodology to highlight the differences among different hydrotreating catalysts based on several physical and chemical properties of the products along with other kinetic constants. PCA is among the disruptive methodologies which can lead to new catalysts or processes for complex problems, together with artificial neural networks [44].

The aim of this work is to apply the PCA methodology to perform a multivariate data analysis of 104 uncorrelated FCC experiments. In particular, to measure the quantitative impact of processing alone or together with VGO: scrap tire pyrolysis oil, high-density polyethylene pyrolysis waxes or dissolved high-density polyethylene. Moreover, this study pursues to analyze on the same grounds the impact of using different experimental conditions (resembling those of industrial units) and using three different equilibrated FCC catalysts (discarded from actual industrial FCC units). The eventual goal is to gather insights into the main key parameters or variables affecting product yields in terms of conversion, octane number, propylene yield or coke formation, among others.

2. Materials and Methods

The variables that have been used in this work are shown in Table 1, categorized into four groups: (i) catalyst properties; (ii) feed properties, (iii) reaction conditions; and (iv) products.

2.1. Catalyst properties

Three equilibrated commercial FCC catalysts based on HY zeolite were used in this study and designated as CAT-1 to -3. These three samples have undergone a steaming treatment in order to equilibrate the catalysts [45].

The textural properties (ST, Sm, SM, Vm and mV) were measured by N_2 adsorption-desorption isotherms at -196 °C using a Micromeritics ASAP 2010 apparatus, after the samples were degassed at 150 °C for 8 h. The zeolite percentage (Z) was calculated using the Johnson correlation [46].

Preprints (www.preprints.org) | NOT PEER-REVIEWED | Posted: 16 October 2018 doi:10.20944/preprints201810.0370.v1

Peer-reviewed version available at Processes 2018, 6, 243; doi:10.3390/pr6120243

Table 1. List of the variables assessed by the principal component analysis.

	Name	Units		Name	Units
Catalysts properties			LPG	Yield of LPG (C_3-C_4)	wt%
ST	BET surface area	$m^2\ g^{-1}$	GL	Yield of gasoline (C_5-C_{12})	wt%
Sm	Micropore area	$m^2\ g^{-1}$	iGL	Gasoline identified	wt%
SM	Matrix or mesopore area	$m^2\ g^{-1}$	LCO	Yield of light cycle oil (C_{13}-C_{20})	wt%
Z	Zeolite percentage	wt%	HCO	Yield of heavy cycle oil (C_{20+})	wt%
Vm	Micropore volume	$cm^3\ g^{-1}$	Ck	Coke content	wt%
mV	Mean pore volume	$cm^3\ g^{-1}$	RON	Octane number (GL)	wt%
Dc	Zeolite cell unit size	Å	A6	Benzene	wt%
Cu	Content of Cu	ppm	A7	Toluene	wt%
Ni	Content of Ni	ppm	A8	Xilenes	wt%
V	Content of V	ppm	A9	Aromatics with 9 carbons	wt%
Fe	Content of Fe	wt%	A10+	Aromatics with 10 carbons	wt%
Na	Content of Na	wt%	AT	Total aromatics	wt%
Al	Content of Al_2O_3	wt%	NT	Total naphthenes	wt%
Re	Content of rare earths Re_2O_3	wt%	P3	Propane	wt%
P	Content of P_2O_5	wt%	P4	Butane	wt%
Ac	Total acidity	$mmol\ g^{-1}$	PT	Total paraffins	wt%
BL	Brönsted-Lewis acid site ratio	$mol\ mol^{-1}$	O3	Propylene	wt%
Feed properties			O4	Butenes	wt%
Pf	Paraffins	wt%	O5	Pentenes	wt%
Of	Olefins	wt%	OT	Total olefins	wt%
Nf	Naphthenes	wt%	IT	Total isoparaffins	wt%
Af	Aromatics	wt%	C3	C_3 hydrocarbons	wt%
Sf	Sulfur	wt%	C4	C_4 hydrocarbons	wt%
Gf	Gasoline (C_5-C_{12})	wt%	C5	C_5 hydrocarbons	wt%
Lf	Light cycle oil (C_{13}-C_{20})	wt%	C6	C_6 hydrocarbons	wt%
Hf	Heavy cycle oil (C_{20+})	wt%	C7	C_7 hydrocarbons	wt%
Reaction conditions			C8	C_8 hydrocarbons	wt%
CO	Catalyst-to-oil ratio	$g\ g^{-1}$	C9	C_9 hydrocarbons	wt%
t	Time	s	C10	C_{10+} hydrocarbons	wt%
T	Temperature	ºC	CT	Total hydrocarbons	wt%
Product properties			iOT	Total isoolefins	wt%
X	Conversion	wt%	nOT	Total linear olefins	wt%
LG	Yield of light gases (C_1-C_2)	wt%	cOT	Total cycloolefins	wt%

The unit cell size (Dc) was obtained from X-ray diffraction (XRD) analysis in a Philips PW 1710 apparatus with a graphite monocromator using CuKα radiation (λ=1.5544 Å). Data were collected using a coupled theta-2theta configuration in the 2–50° range with a step size of 0.02 and a scan time of 1 s. The acidity (Ac) was measured through temperature programmed desorption (TPD) of NH_3 adsorbed at 150 °C in a TG-DSC Setaram 111 calorimeter, which is connected on-line with a Balzers Quadstar 422 mass spectrometer. The Brönsted-Lewis acid site ratio (BL) was obtained using Fourier transformed infrared (FTIR) spectrometry of adsorbed pyridine in a Nicolet 6700 FTIR apparatus with a catalytic SPECAC chamber. The elemental analysis (Cu, Ni, V, Fe, Na, Al, Re and P) was carried out by Inductively Coupled Plasma-Atomic Emission Spectroscopy (ICP-AES) using a X7-II Thermo quadrupolar mass spectrometer (QICP- MS), previously subjecting the fresh catalysts to acid digestion with HF (Merck) at 90 °C.

2.2. Feed properties

A total of six feeds were used: (1) vacuum gas oil, VGO; (2) high-density polyethylene (HDPE) pyrolysis waxes, PW; (3) scrap tire pyrolysis oil, STPO; (4) VGO+HDPE, 95 wt% +5 wt%; (5) VGO+PW, 80 wt% + 20 wt%; (6) VGO+STPO, 80 wt% + 20 wt%. VGO was provided by Petronor S.A. (Muskiz, Spain), API gravity of 21.1 and viscosity at 100 °C of 8.6 cSt. Pre-grinded particles of < 1 mm of HDPE were provided by Dow Chemical (Tarragona, Spain), with an average molecular weight of 46,200 g mol^{-1} and a polydispersity of 2.89.

the PW and STPO The pyrolysis of HDPE or tires – previously grinded to particles of < 1 mm, after removal of textile reinforcements and metallic components provided by Jenecan S.L. (Abanto-Zierbana, Spain)– was performed in a conical spouted bed reactor under the following conditions for (i) HDPE (continuous flow regime): 500 °C, HDPE flow rate of 1 g min^{-1}, N_2 flow rate of 7.5 L min^{-1}, and 30 g of sand ($0.63 < d_p < 1$ mm) in the bed [47]; and (ii) tires (semi-continuous regime): 500 °C, tire feed of 2 g per run, N_2 flow rate of 6.5 L min^{-1}, and 30 g of sand ($0.63 < d_p < 1$ mm) in the bed [48], in order to provide , respectively.

The fractions of the feed (Gf, Lf and Hf) were analyzed by simulated distillation, according to the ASTM D-2887 standard, in an Agilent 6890 Series GC gas chromatograph. In order to carry out the simulated distillation of PW, this feed was diluted in tetrahydrofuran (THF) at 55 °C in a TTHF mass ratio of 1:2. The amount of Sulfur (Sf) was analyzed by gas chromatography in an Agilent Technologies 7890A setup connected in line and provided with an FID detector and a pulsed flame photometric detector (PFPD). Additionally, the chemical composition (Pf, Of, Nf and Af) analysis was performed in a bi-dimensional Agilent 7890A gas chromatograph (GC×GC) provided with two columns and a flow modulator, coupled in line with an Agilent 5975C Series mass spectrometer (MS) and a flame ionization detectors (FID), additional details can be found elsewhere [22].

2.3. Reaction conditions and product properties

The FCC runs were carried out in a CREC (Chemical Reactor Engineering Centre) riser simulator, using reaction condition resembling those of industrial FCC units [49]: T, 500-530-560 °C; CO, 3-5-7 g g^{-1}; t, 3-6-12 s. A detailed schematization of the reactor is described in a previous work [24]. Once the reaction time was completed, the products were withdrawn from the reactor by triggering a valve which connects the reactor with a vacuum chamber in order to avoid side reactions.

The reaction products that are gases in the reaction conditions were analyzed through the same GC described before for the analysis of Sf. The coke content (Ck) was determined by combustion in a TA Instruments TGA-Q 5000 thermobalance, applying a temperature ramp 300-550 °C, at a 3 °C min^{-1} rate. The conversion (X_i) has been defined as the fraction of the feed that yields the most important products (LG + LPG + GL + Ck). The research octane number (RON) was calculated from a method established by Anderson et al. [50] and based on the composition of the GL fraction measured by gas chromatography.

2.4. Principal component analysis (PCA)

A routine has been developed in MATLAB™ for the multivariate analysis of the experimental results. The dataset X was configured as a matrix consisting of *n* columns (for *n* variables) and *m* rows (for *m* number of independent experiments). Each of the variables is an independent or dependent one and is summarized within Table 1.

$$X = \begin{bmatrix} x_{11} & x_{12} & \dots & x_{1n} \\ x_{21} & x_{22} & \dots & x_{2n} \\ \dots & & & \\ x_{m1} & x_{m2} & \dots & x_{mn} \end{bmatrix} \quad (1)$$

The data has been normalized with the command *normc*. Then, the data matrix X has been decomposed into a score vector t_i and a loading vector p_i with a residual error *E*, as:

$$X = t_1 p_1^T + t_2 p_2^T + \dots + t_k p_k^T + E \quad (2)$$

The correlations of the variables were obtained by first calculating the covariance (*cov* command) and then transforming it to a correlation matrix (*corrcov* command). The covariance matrix can also be expressed as:

$$R = \sum_{j=1}^{n} p_j \lambda_j p_j^T = P \Lambda P^T \quad (3)$$

Where P is a *mxn* matrix of eigenvectors and Λ is a matrix of eigenvalues associated to those eigenvectors, as:

$$\Lambda = \begin{bmatrix} \lambda_1 & 0 & \dots & 0 \\ 0 & \lambda_2 & 0 & 0 \\ \dots & \dots & \dots & \dots \\ 0 & 0 & 0 & \lambda_n \end{bmatrix} \quad (4)$$

The eigenvalues and eigenvectors (calculated with *eig*) are used for the calculation of the principal components of the correlation matrix. To compute the loadings of each PC, the eigenvectors were multiplied by the square root of the eigenvalues diagonal matrix (Eq. 4). The eigenvalues also allow for the calculation of the portion of the total variance associated with the *j*-th eigenvalue:

$$\nu_j = \frac{\lambda_j}{\sum_j \lambda_j} \quad (5)$$

In addition, the Varimax rotation was applied to facilitate the interpretation of the results and was calculated using the command *rotatefactors* over the loading matrix. The command *pca* was used to obtain the score matrix and *zscore* to obtain the z-score matrix.

3. Results

3.1. Properties of the catalysts and feeds

Some of the main properties of the catalysts are summarized in Figure 1: ST, Sm, SM, Ac and BL. These results of Figure 1 illustrate that all features of the studied catalysts correspond to those typical of industrial FCC ones: ST of 124-190 $m^2 g^{-1}$; Sm of 63-139 $m^2 g^{-1}$; Ac of 0.04-0.12 mmol g^{-1}; and BL of 0.6-1.56.

CAT-1 is a spent catalyst, that has been discarded from an industrial FCC unit and, as such, it has relatively low ST, Ac and BL values. This is due to the degradation of CAT-1 suffered in process conditions. CAT-2 has a relatively high content of ST due to a greater proportion of zeolite (Z) and intermediate value of Ac and BL, indicating that this catalyst aims for the conversion of relatively "light" feeds (avoiding over cracking) and an increase in the olefin content and octane number of the

Preprints (www.preprints.org) | NOT PEER-REVIEWED | Posted: 16 October 2018 doi:10.20944/preprints201810.0370.v1

Peer-reviewed version available at Processes 2018, 6, 243; doi:10.3390/pr6120243

products. On the other hand, CAT-3 has the lowest Sm value and the greatest Ac and BL values, indicating that this catalyst aims for the "high conversion" of relatively "heavy" feeds (promoting the cracking of bulky molecules).

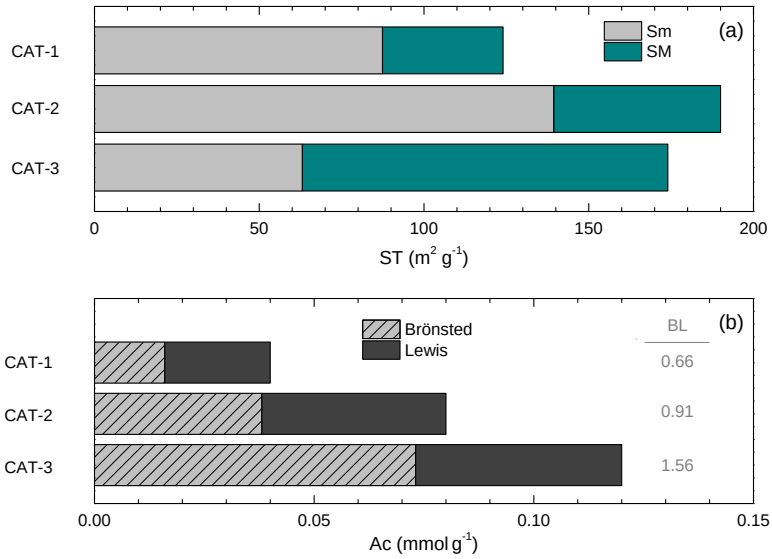

Figure 1. Main properties of the catalysts employed, CAT-1 to -3, in terms of (a) textural and (b) acidic properties.

The elemental analysis of the catalysts shows contents of Ni (741 ppm) and V (3335 ppm) one order of magnitude higher for the CAT-1 than these for CAT-2 and -3, again indicating the spent nature of CAT-1. The rest of the compositions are relatively similar (Cu, Fe, Na and Al) except for the Re that are 2.50, 0.86 and 1.35 wt% for CAT-1 to -3, respectively.

Figure 2 displays the composition of the six feeds studied. All the feeds (with the exception of STPO) consist primarily of an HCO (Hf) fraction with concentrations of 82.0-95.5 wt%. STPO, on the other hand, presents a significantly higher content of LCO (Lf, 29.3 wt%) and gasoline (Gf, 15.5 wt%), as a consequence of the thermal non-selective cracking that occur in the pyrolysis process, which leads to a product distribution towards lighter components and a low concentration of heavy hydrocarbons [51,52].

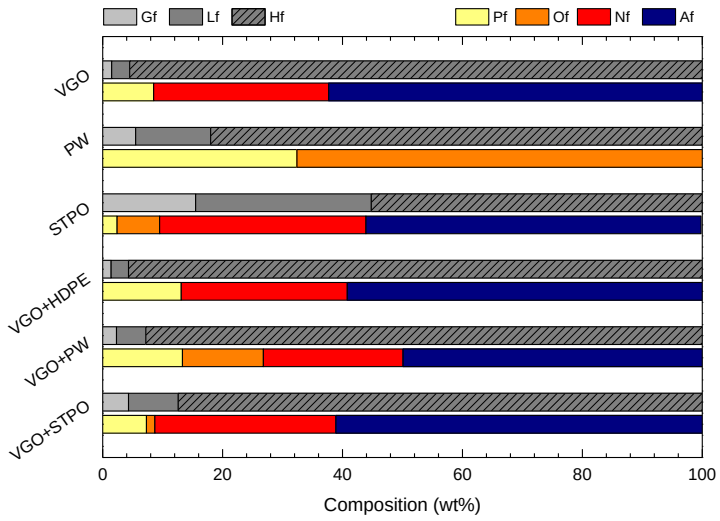

Preprints (www.preprints.org) | NOT PEER-REVIEWED | Posted: 16 October 2018 doi:10.20944/preprints201810.0370.v1

Peer-reviewed version available at Processes 2018, 6, 243; doi:10.3390/pr6120243

Figure 2. Composition (wt%) in terms of fractions (Gf, Lf and Hf) and lumps (Pf, Of, Nf and Af) for all the feeds used in this study. Detailed designations for the different fractions and lumps can be found in Table 1.

Regarding their chemical composition, and while waxes consist only in linear paraffins (32.4 wt%) and olefins (67.6 wt%), the rest of the feeds are relatively similar in their chemical nature with an overall predominance of cyclic unsaturated (50.0-62.4 wt% aromatics) and saturated compounds (23.3-34.4 wt% naphthenes).

3.2. Multivariate analysis

From the experimental data consisting in 104 uncorrelated runs, a total of 11 PCs were extracted. PC1, PC2 and PC3 characterize 59.22% of the variance, and therefore have been used for the main discussion onwards. Figure 3 shows the score plot of the three main PCs: the experimental data is homogenously distributed along PC2-3, and therefore clustering, outliers and other unwanted patterns in this framework can be discarded. However, when the experiments are discretized based on feed types, a clustering behavior is observed along PC1.

The type and characteristics of the feed are observed to be strongly correlated with PC1 and PC3 and with little influence of PC2. The results of the cracking of STPO show the highest scores along the PC1 whereas the experimental results of the cracking of VGO have the lowest scores along the PC3 (not making a proper cluster). In relation with Figure 2, this trend of scores is related with the amount of HCO in the feed (Hf, which is particularly high for VGO and HDPE+VGO feeds, and relatively low for STPO. Indeed, the distinctive composition of the STPO (much lighter than the rest of feeds) is responsible of the certain degree of clustering observed in the score plot of the cracking results (Figure 3). All in all, these results reveal that the composition of the feed should play an important role on the loadings of PC1.

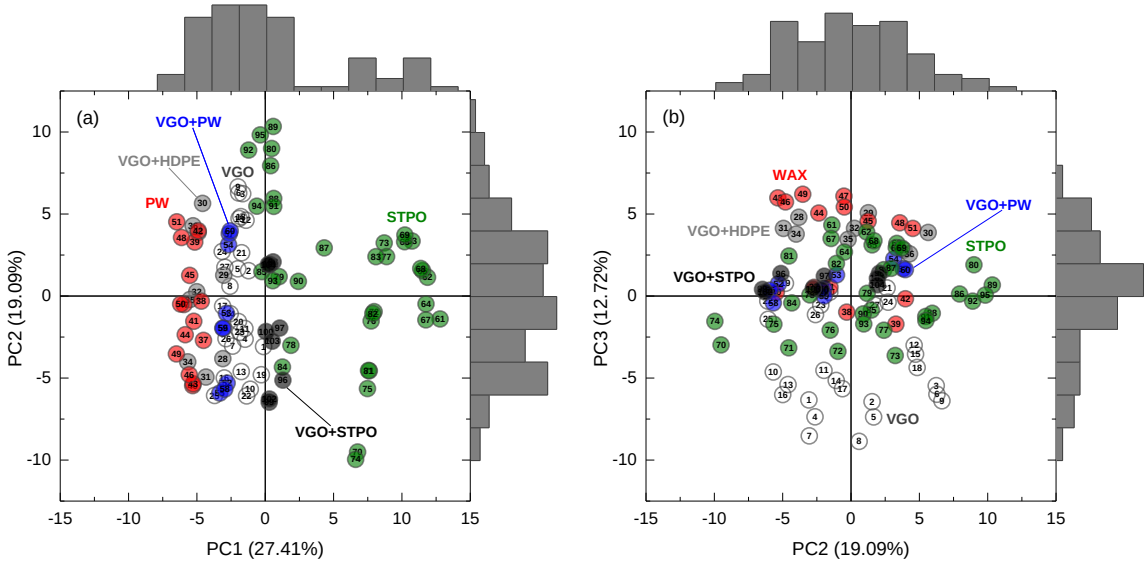

Figure 3. Score plot for 104 uncorrelated runs in terms of (a) PC1 vs. PC2 and (b) PC2 vs. PC3. The bars of the plots correspond to the histograms of the projections in each PC.

Figure 4 displays the Varimax loading plots for PC1-PC2 (Figure 2a) and PC2-PC3 (Figure 2b). This graph also shows zooms of different sections of the PC1-PC2 (Figures 2c and 2d) and PC2-PC3 (Figures 2e and 2f) representations.

The composition of the feed is strongly correlated with PC1, which describes 27.41% of the variance. The "negative" fractions of the feed, in PC1, are HCO (Hf) and paraffins (Pf) which are, hence, the least reactive fractions . On the contrary, gasoline (Gf) and LCO (Lf) are "positive" fractions because they are at the opposite side of the least reactive ones. Figure 4a indicates that there is a

correlation (or proximity) between the HCO in the feed (Hf) and that of the products (HCO) and (LCO) indicating one of the main pathways of reaction: HCO (unreacted) and HCO → LCO. Paraffins in the feed (Pf) are correlated with isoparaffins (IT) indicating the participance of isomerization reactions in the cracking mechanisms. On the other side of the PC1 (Figure 4a), naphthenes in the feed (Nf) are linked with the cycloolefins (naphthenes with double bounds, cOT), indicating the partial dehydrogenation of the cyclohexane and cyclopentane rings (most likely in Nf).

Based on their loadings, the distribution of boiling point fractions of the feed (Hf, Gf or Lf) has a stronger impact on process performance than its chemical composition (Pf, Of, Af or Nf). Besides, a cluster of points is observed on the left side of Figure 4a, which has been zoomed in Figure 4c. The "positive" fractions of the feed such as Lf and Gf are primarily converted into gasoline products (GL) with a high content of C_{7-9} hydrocarbons in the form of aromatics (AT). In particular, we observe relatively high loadings within PC1 for benzene (A6), toluene (A7), xylenes (A8) and C_{9+} alkyl aromatics, while also naphthenes (NT). These results illustrate the transformation of alkylated naphthenes (Nf) and aromatics (Af) present in the gasoline (Gf) and LCO (Lf) into less alkylated aromatics, contained in the produced gasoline (GL). It is worth mentioning that the variables describing process conditions and catalyst properties have very low impact, expressed as low loadings along PC1. The critical role of feed composition on the overall performance of the FCC process has been recurrently indicated before [12,24,28,53].

The process conditions are strongly correlated with PC2, which describes 19.09% of the variance. The three operational conditions (CO, t and T) are on one side of the plot because increasing each of those leads to an increase of severity of operation with higher cracking conversion. Within the conditions studied here, the trend of variables in increasing order of influence in the process are: catalyst-to-oil ratio (CO) < time (t) < temperature (T). A cluster of points is observed on the lower side of Figure 4a, which has been zoomed in Figure 4d. Time (t) strongly influences the content of coke (Ck) and octane number (RON). Some paraffins such as (P3, P4 and PT) are linked with PC2, as a result of the higher predominance of hydrogen transfer reactions at more severe process conditions. Temperature (T) influences the quality of the products, in terms of olefin content and RON, and quantity of the lighter fractions such as LPG and LG. Attention should be placed on the fact that olefins (OT) and propylene (O3), which is one of the most important products in the FCC, is more influenced by the process conditions (PC2) and T in particular, than the feed properties (PC1). These observations have already been reported by Ibarra et al. [28] for the catalytic cracking of VGO+bio-oil blends. Specifically, temperature has a greater impact in the formation of gas products (LPG and LG) by favoring cracking reactions, in particular the extent of each type of reaction (monomolecular, bimolecular, etc.) [54]. Furthermore, T is also known to heavily determine the total yield of olefins in the products as a consequence of paraffin dehydrogenation reactions being favored [55,56].

The catalyst properties are strongly correlated with PC3, which describes 12.72% of the variance. Among the dependent products, only the coke content (Ck) seems to be affected by the catalyst properties. At the same time, Ck has a null loading of PC1 related with feed properties and significant loading of PC2 related with process conditions, in particular related with time. This behavior of coke demonstrated the significant impact of reaction time on coke formation [30].

The catalyst properties show two clusters of points along PC3, which have been zoomed in Figures 4e and 4f. In this case, the main correlated properties to Ck are those concerning acidity and textural features (Figure 4e), in the following order: Ac > mV > BL > SM >> SM, Fe >> Al. Thus, among the catalyst properties, acidity descriptors are the ones that should be primarily considered for the modeling of cracking reactions [57]. Inversely, on the opposite side of PC3 (Figure 4f), the variables of the catalyst found present the following loading trend: P > Na > Ni ≈ V >> Re. These elements, and specifically the first four, are then correlated with the decrease of acidity in the original catalyst or the spent one.

Preprints (www.preprints.org) | NOT PEER-REVIEWED | Posted: 16 October 2018 doi:10.20944/preprints201810.0370.v1

Peer-reviewed version available at Processes 2018, 6, 243; doi:10.3390/pr6120243

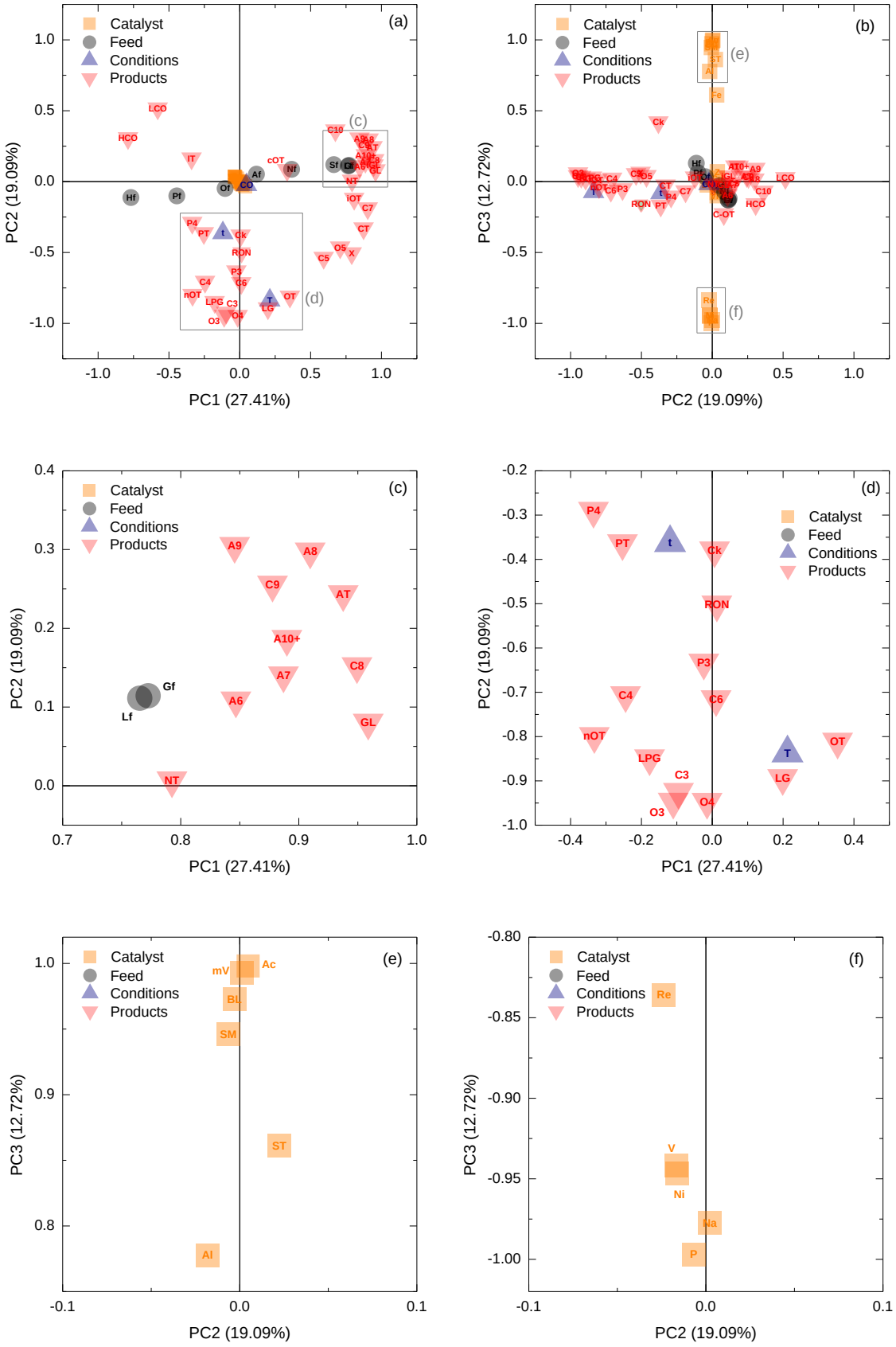

Figure 4. Varimax loading plots for the (a) PC1 vs. PC2 and (b) PC2 vs. PC3. Graphs (c, d) and (e, f) correspond to zoomed areas of graphs (a) and (b), respectively.

4. Conclusions

We have tested the principal component analysis (PCA) over a set of 104 uncorrelated fluid catalytic cracking (FCC) runs using different waste feeds, catalysts and operation conditions. This approach has proven to be suitable for assessing the impact of 64 variables categorized as feed, process, catalyst and product properties.

The results show that each category of independent variables (feed, process and catalyst properties) has been correlated with a single principal component (PC) in such a way that the percentage of the total variance assigned to those categories results as: PC1, related with feed properties explains 27.41% of the variance; PC2, process conditions, 19.09%; PC3, catalyst properties, 12.72%.

- Among the feed properties, the lump fraction with more than 20 carbons is the one affecting the most the yields of cycle oils (detrimental to the FCC performance) whereas the fraction with less than 20 carbons is correlated with the amount and aromatic content of gasoline. The chemical composition of the feed is of lesser relevance than its boiling point distribution.
- Among the process conditions, the key variables are predominantly time and temperature, which are strongly correlated with the amount and olefin content of the lighter fractions (dry and liquified petroleum gases, with attention to propylene).
- Among the catalyst properties, two sets of variables have been obtained: those positively affecting the FCC performance, such as acidity and micropore area, and on the other hand detrimental variables, as the content of P, Na, V or Ni.

This multivariate analysis can provide insight from both an analytical and compositional perspective, greatly simplifying highly complex FCC conversion processes, and thus presenting high industrial relevance.

Author Contributions: conceptualization and project administration, P.C.; methodology and supervision, J.M.A and P.C.; validation, investigation, data curation and formal analysis; J.I.A, I.H and E.R.

Funding: This research was funded by the Ministry of Economy and Competitiveness (MINECO) of the Spanish Government (CTQ2015-67425R and CTQ2016-79646-P), the European Regional Development Funds (ERDF) and the Basque Government (IT748-13). Dr. Hita is grateful for her postdoctoral grant awarded by the Department of Education, University and Research of the Basque Government (POS_2015_1_0035). Dr. Rodriguez is thankful to the University of the Basque Country UPV/EHU (Zabalduz Programme).

Conflicts of Interest: The authors declare no conflict of interest.

References

1. Charpentier, J. C. In the frame of globalization and sustainability, process intensification, a path to the future of chemical and process engineering (molecules into money). *Chem. Eng. J.* **2007**, *134*, 84–92, doi:10.1016/j.cej.2007.03.084.
2. Gao, X.; Shang, C.; Jiang, Y.; Huang, D.; Chen, T. Refinery scheduling with varying crude: A deep belief network classification and multimodel approach. *AIChE J.* **2014**, *60*, 2525–2532, doi:10.1002/aic.14455.
3. Yang, S.; Wang, N. A P systems based hybrid optimization algorithm for parameter estimation of FCCU reactor-regenerator model. *Chem. Eng. J.* **2012**, *211–212*, 508–518, doi:10.1016/j.cej.2012.08.040.
4. Letzsch, W. Fluid Catalytic Cracking (FCC) in Petroleum Refining. In *Handbook of Petroleum Processing*; Treese, A. S., Pujadó, R. P., Jones, J. D. S., Eds.; Springer International Publishing: Cham, 2015; pp. 261–316 ISBN 978-3-319-14529-7.
5. Chen, Y. M. Recent advances in FCC technology. *Powder Technol.* **2006**, *163*, 2–8, doi:10.1016/j.powtec.2006.01.001.
6. Fogassy, G.; Thegarid, N.; Schuurman, Y.; Mirodatos, C. The fate of bio-carbon in FCC co-processing products. *Green Chem.* **2012**, *14*, 1367–1371, doi:10.1039/c2gc35152h.

7. Zhang, Y.; Brown, T. R.; Hu, G.; Brown, R. C. Techno-economic analysis of two bio-oil upgrading pathways. *Chem. Eng. J.* **2013**, doi:10.1016/j.cej.2013.01.030.
8. Corma, A.; Corresa, E.; Mathieu, Y.; Sauvanaud, L.; Al-Bogami, S.; Al-Ghrami, M. S.; Bourane, A. Crude oil to chemicals: Light olefins from crude oil. *Catal. Sci. Technol.* **2017**, *7*, 12–46, doi:10.1039/c6cy01886f.
9. Vogt, E. T. C.; Weckhuysen, B. M. Fluid catalytic cracking: recent developments on the grand old lady of zeolite catalysis. *Chem. Soc. Rev.* **2015**, *44*, 7342–7370, doi:10.1039/c5cs00376h.
10. Corma, A.; Sauvanaud, L. FCC testing at bench scale: New units, new processes, new feeds. *Catal. Today* **2013**, *218–219*, 107–114, doi:10.1016/j.cattod.2013.03.038.
11. Arandes, J. M.; Torre, I.; Azkoiti, M. J.; Ereña, J.; Olazar, M.; Bilbao, J. HZSM-5 zeolite as catalyst additive for residue cracking under FCC conditions. *Energy Fuels* **2009**, *23*, 4215–4223, doi:10.1021/ef9002632.
12. Arandes, J. M.; Torre, I.; Azkoiti, M. J.; Ereña, J.; Bilbao, J. Effect of atmospheric residue incorporation in the fluidized catalytic cracking (FCC) feed on product stream yields and composition. *Energy Fuels* **2008**, *22*, 2149–2156, doi:10.1021/ef800031x.
13. García, J. R.; Falco, M.; Sedran, U. Intracrystalline mesoporosity over Y zeolites. Processing of VGO and resid-VGO mixtures in FCC. **2017**, doi:10.1016/j.cattod.2017.04.010.
14. Passamonti, F. J.; Sedran, U. Recycling of waste plastics into fuels. LDPE conversion in FCC. *Appl. Catal. B Environ.* **2012**, *125*, 499–506, doi:10.1016/j.apcatb.2012.06.020.
15. Odjo, A. O.; García, A. N.; Marcilla, A. Conversion of low density polyethylene into fuel through co-processing with vacuum gas oil in a fluid catalytic cracking riser reactor. *Fuel Process. Technol.* **2013**, *113*, 130–140, doi:10.1016/j.fuproc.2013.03.008.
16. Torre, I.; Arandes, J. M.; Castaño, P.; Azkoiti, M. J.; Bilbao, J.; de Lasa, H. I. Catalytic Cracking of Plastic Pyrolysis Waxes with Vacuum Gasoil: Effect of HZSM-5 Zeolite in the FCC Catalyst. *Int. J. Chem. React. Eng.* 2006, *4*.
17. Arandes, J. M. M.; Azkoiti, M. J. J.; Torre, I.; Olazar, M.; Castaño, P. Effect of HZSM-5 catalyst addition on the cracking of polyolefin pyrolysis waxes under FCC conditions. *Chem. Eng. J.* **2007**, *132*, 17–26, doi:10.1016/j.cej.2007.01.012.
18. Arandes, J. M. M.; Torre, I.; Azkoiti, M. J. J.; Castaño, P.; Bilbao, J.; de Lasa, H. Effect of catalyst properties on the cracking of polypropylene pyrolysis waxes under FCC conditions. *Catal. Today* **2008**, *133*, 413–419, doi:10.1016/j.cattod.2007.12.080.
19. Arandes, J. M.; Torre, I.; Castaño, P.; Olazar, M.; Bilbao, J. Catalytic cracking of waxes produced by the fast pyrolysis of polyolefins. *Energy Fuels* **2007**, *21*, 561–569, doi:10.1021/ef060471s.
20. Lovás, P.; Hudec, P.; Jambor, B.; Hájeková, E.; Horňáček, M. Catalytic cracking of heavy fractions from the pyrolysis of waste HDPE and PP. *Fuel* **2017**, *203*, 244–252, doi:10.1016/j.fuel.2017.04.128.
21. Hita, I.; Rodríguez, E.; Olazar, M.; Bilbao, J.; Arandes, J. M. M.; Castaño, P. Prospects for Obtaining High Quality Fuels from the Hydrocracking of a Hydrotreated Scrap Tires Pyrolysis Oil. *Energy Fuels* **2015**, *29*, 5458–5466, doi:10.1021/acs.energyfuels.5b01181.
22. Hita, I.; Gutiérrez, A.; Olazar, M.; Bilbao, J.; Arandes, J. M. J. M. J. M.; Castaño, P. Upgrading model compounds and Scrap Tires Pyrolysis Oil (STPO) on hydrotreating NiMo catalysts with tailored supports. *Fuel* **2015**, *145*, 158–169.
23. Cordero-Lanzac, T.; Hita, I.; Veloso, A.; Arandes, J. M.; Rodríguez-Mirasol, J.; Bilbao, J.; Cordero, T.; Castaño, P. Characterization and controlled combustion of carbonaceous deactivating species deposited on an activated carbon-based catalyst. *Chem. Eng. J.* **2017**, *327*, 454–464, doi:10.1016/j.cej.2017.06.077.
24. Errekatxo, A.; Ibarra, A.; Gutierrez, A.; Bilbao, J.; Arandes, J. M.; Castaño, P. Catalytic deactivation

pathways during the cracking of glycerol and glycerol/VGO blends under FCC unit conditions. *Chem. Eng. J.* **2017**, *307*, 955–965, doi:https://doi.org/10.1016/j.cej.2016.08.100.

25. Pinho, A. de R.; de Almeida, M. B. B.; Mendes, F. L.; Ximenes, V. L.; Casavechia, L. C. Co-processing raw bio-oil and gasoil in an FCC Unit. *Fuel Process. Technol.* **2015**, *131*, 159–166, doi:https://doi.org/10.1016/j.fuproc.2014.11.008.
26. Ma, W.; Liu, B.; Zhang, R.; Gu, T.; Ji, X.; Zhong, L.; Chen, G.; Ma, L.; Cheng, Z.; Li, X. Co-upgrading of raw bio-oil with kitchen waste oil through fluid catalytic cracking (FCC). *Appl. Energy* **2018**, *217*, 233–240, doi:10.1016/J.APENERGY.2018.02.036.
27. Wang, Y.; Cao, Y.; Li, J. Preparation of biofuels with waste cooking oil by fluid catalytic cracking: The effect of catalyst performance on the products. *Renew. Energy* **2018**, *124*, 34–39, doi:10.1016/J.RENENE.2017.08.084.
28. Ibarra, Á.; Rodríguez, E.; Sedran, U.; Arandes, J. M.; Bilbao, J. Synergy in the Cracking of a Blend of Bio-oil and Vacuum Gasoil under Fluid Catalytic Cracking Conditions. *Ind. Eng. Chem. Res.* **2016**, doi:10.1021/acs.iecr.5b04502.
29. Bertero, M.; Puente, G. D. La; Sedran, U. Products and coke from the conversion of bio-oil acids, esters, aldehydes and ketones over equilibrium FCC catalysts. *Renew. Energy* **2013**, *60*, 349–354, doi:10.1016/j.renene.2013.04.017 Technical note.
30. Ibarra, Á.; Veloso, A.; Bilbao, J.; Arandes, J. M. J. M.; Castaño, P. Dual coke deactivation pathways during the catalytic cracking of raw bio-oil and vacuum gasoil in FCC conditions. *Appl. Catal. B Environ.* **2016**, *182*, 336–346, doi:10.1016/j.apcatb.2015.09.044.
31. Bezergianni, P. S.; Dimitriadis, A.; Kikhtyanin, O.; Kubi Cka, D. Refinery co-processing of renewable feeds. **2018**, doi:10.1016/j.pecs.2018.04.002.
32. Feital, T.; Kruger, U.; Dutra, J.; Pinto, J. C.; Lima, E. L. Modeling and performance monitoring of multivariate multimodal processes. *AIChE J.* **2013**, *59*, 1557–1569, doi:10.1002/aic.13953.
33. Rato, T.; Reis, M.; Schmitt, E.; Hubert, M.; De Ketelaere, B. A systematic comparison of PCA-based Statistical Process Monitoring methods for high-dimensional, time-dependent Processes. *AIChE J.* **2016**, *62*, 1478–1493, doi:10.1002/aic.15062.
34. Tomita, R. K.; Park, S. W.; Sotomayor, O. A. Z. Analysis of activated sludge process using multivariate statistical tools - A PCA approach. *Chem. Eng. J.* **2002**, *90*, 283–290, doi:10.1016/S1385-8947(02)00133-X.
35. Zhang, J.; Martin, E. B.; Morris, A. J. Process monitoring using non-linear statistical techniques. *Chem. Eng. J.* **1997**, *67*, 181–189, doi:10.1016/S1385-8947(97)00048-X.
36. Gregersen, L.; Jørgensen, S. B. Supervision of fed-batch fermentations. *Chem. Eng. J.* **1999**, doi:10.1016/S1385-8947(99)00018-2.
37. Kashani, M. N.; Shahhosseini, S. A methodology for modeling batch reactors using generalized dynamic neural networks. *Chem. Eng. J.* **2010**, *159*, 195–202, doi:10.1016/j.cej.2010.02.053.
38. Sjögren, M.; Li, H.; Rannug, U.; Westerholm, R. A multivariate statistical analysis of chemical composition and physical characteristics of ten diesel fuels. *Fuel* **1995**, *74*, 983–989, doi:10.1016/0016-2361(95)00056-B.
39. Pasadakis, N.; Yiokari, C.; Varotsis, N.; Vayenas, C. Characterization of hydrotreating catalysts using the principal component analysis. *Appl. Catal. A Gen.* **2001**, *207*, 333–341, doi:10.1016/S0926-860X(00)00673-6.
40. Mostad, H. B.; Riis, T. U.; Ellestad, O. H. Use of principal component analysis in catalyst characterization. Catalytic cracking of decalin over Y-zeolites. *Appl. Catal.* **1990**, *64*, 119–141, doi:10.1016/S0166-9834(00)81557-2.
41. Héberger, K.; Németh, A.; Cotarca, L.; Delogu, P. Principal component analysis of data on the catalytic

oxidation of toluene. *Appl. Catal. A Gen.* **1994**, *119*, L7–L12, doi:10.1016/0926-860X(94)85019-4.

42. Aguado, R.; Elordi, G.; Arrizabalaga, A.; Artetxe, M.; Bilbao, J.; Olazar, M. Principal component analysis for kinetic scheme proposal in the thermal pyrolysis of waste HDPE plastics. *Chem. Eng. J.* **2014**, *254*, 357–364, doi:10.1016/j.cej.2014.05.131.
43. Aguado, R.; Arrizabalaga, A.; Arabiourrutia, M.; Lopez, G.; Bilbao, J.; Olazar, M. Principal component analysis for kinetic scheme proposal in the thermal and catalytic pyrolysis of waste tyres. *Chem. Eng. Sci.* **2014**, *106*, 9–17, doi:http://dx.doi.org/10.1016/j.ces.2013.11.024.
44. Li, H.; Zhang, Z.; Liu, Z. Application of Artificial Neural Networks for Catalysis: A Review. *Catalysts* **2017**, *7*, 306, doi:10.3390/catal7100306.
45. Tonetto, G. M.; Ferreira, M. L.; Atias, J. A.; De Lasa, H. I. Effect of steaming treatment in the structure and reactivity of FCC catalysts. *AIChE J.* **2006**, *52*, 754–768, doi:10.1002/aic.10629.
46. JOHNSON, M. Estimation of the zeolite content of a catalyst from nitrogen adsorption isotherms. *J. Catal.* **1978**, *52*, 425–431, doi:10.1016/0021-9517(78)90346-9.
47. Elordi, G.; Olazar, M.; Lopez, G.; Artetxe, M.; Bilbao, J. Product Yields and Compositions in the Continuous Pyrolysis of High-Density Polyethylene in a Conical Spouted Bed Reactor. *Ind. Eng. Chem. Res* **2011**, *50*, 6650–6659, doi:10.1021/ie200186m.
48. Arabiourrutia, M.; Lopez, G.; Elordi, G.; Olazar, M.; Aguado, R.; Bilbao, J. Product distribution obtained in the pyrolysis of tyres in a conical spouted bed reactor. *Chem. Eng. Sci.* **2007**, *62*, 5271–5275, doi:http://dx.doi.org/10.1016/j.ces.2006.12.026.
49. Al-Sabawi, M.; De Lasa, H. Kinetic modeling of catalytic conversion of methylcyclohexane over USY zeolites: Adsorption and reaction phenomena. *AIChE J.* **2009**, *55*, 1538–1558, doi:10.1002/aic.11825.
50. Anderson, J. E.; Kramer, U.; Mueller, S. A.; Wallington, T. J. Octane Numbers of Ethanol− and Methanol−Gasoline Blends Estimated from Molar Concentrations. *Energy Fuels* **2010**, *24*, 6576–6585, doi:10.1021/ef101125c.
51. Arabiourrutia, M.; Olazar, M.; Aguado, R.; López, G.; Barona, A.; Bilbao, J. HZSM-5 and HY Zeolite Catalyst Performance in the Pyrolysis of Tires in a Conical Spouted Bed Reactor. *Ind. Eng. Chem. Res.* **2008**, *47*, 7600–7609, doi:10.1021/ie800376d.
52. Olazar, M.; Aguado, R.; Arabiourrutia, M.; Lopez, G.; Barona, A.; Bilbao, J. Catalyst Effect on the Composition of Tire Pyrolysis Products. *Energy Fuels* **2008**, *22*, 2909–2916, doi:10.1021/ef8002153.
53. Torre, I.; Arandes, J. M.; Azkoiti, M. J.; Olazar, M.; Bilbao, J. Cracking of coker naphtha with gas-oil. Effect of HZSM-5 zeolite addition to the catalyst. *Energy Fuels* **2007**, *21*, 11–18, doi:10.1021/ef060344w.
54. Li, J.; Li, T.; Ma, H.; Sun, Q.; Li, C.; Ying, W.; Fang, D. Kinetics of coupling cracking of butene and pentene on modified HZSM-5 catalyst. *Chem. Eng. J.* **2018**, *346*, 397–405, doi:10.1016/j.cej.2018.04.061.
55. He, S.; Li, J.; Wang, B.; Dai, X.; Sun, C.; Bai, Z.; Guo, Q.; Seshan, K. Metals modification of the paraffin dehydrogenation catalyst regenerated by coke combustion. *Appl. Catal. A Gen.* **2016**, *513*, 82–88, doi:https://doi.org/10.1016/j.apcata.2015.12.027.
56. Bhasin, M. M.; McCain, J. H.; Vora, B. V.; Imai, T.; Pujadó, P. R. Dehydrogenation and oxydehydrogenation of paraffins to olefins. *Appl. Catal. A Gen.* 2001, *221*, 397–419.
57. Van Borm, R.; Reyniers, M.-F.; Marin, G. B. Catalytic cracking of alkanes on FAU: Single-event microkinetic modeling including acidity descriptors. *AIChE J.* **2012**, *58*, 2202–2215, doi:10.1002/aic.13831.